

Electrodeposition of δ -phase based Cu-Sn mirror alloy from sulfate-aqueous electrolyte for solar reflector application

Sherine Alex^{a,b}, Bikramjit Basu^{a,c}, Sanchita Sengupta^a, Upendra K. Pandey^a, Kamanio Chattopadhyay^{a,d,*}

^a Interdisciplinary Centre for Energy Research, Indian Institute of Science, Bangalore, India.

^b Centre for Nanoscience and Engineering, Indian Institute of Science, Bangalore, India.

^c Materials Research Centre, Indian Institute of Science, Bangalore, India.

^d Materials Engineering, Indian Institute of Science, Bangalore, India.

Email: kamanio@materials.iisc.ernet.in

Keywords: Cu-Sn intermetallics, electrodeposition, solar reflector

Abstract

Copper-tin (Cu-Sn) intermetallic alloy coating was developed on mild steel substrate by galvanostatic electrodeposition technique from sulfate-based acidic electrolyte containing Laprol as additive. The homogenous coating containing cubic δ phase with composition of 32.6 % Sn was obtained, when a current of -8.5 mA was made to flow through the electrochemical bath. The optimized coating with thickness of $\sim 0.4 - 3 \mu\text{m}$ exhibits $\sim 80\%$ specular reflectance. The coating has a hardness of 2.6 GPa, suggesting a good scratch resistance property. The experimental results also suggest that the hydrophobic surface of Cu-32.6% Sn thin film can be potentially used as an attractive coating for solar reflector application under dusty and humid conditions.

1. Introduction

In the last decade, extensive efforts are invested to develop and improve technologies to harvest energy from renewable sources led to development and improvement of several technologies. Utilisation of solar energy is central to most of these efforts. Although photovoltaic conversion has technologically matured rapidly, ‘Concentrating Solar Power

(CSP) technology', still represents one of the most promising and affordable solar technologies where, sunlight is converted into higher or lower grade thermal energy [1]. An increasing number of CSP plants have been constructed in the last decades [2] towards fulfilling our growing energy demand and a further growth for this renewable technology is envisaged in coming future.

Briefly, CSP [3] technology utilizes parabolic troughs, solar towers, and parabolic dishes to concentrate the solar energy using reflective surfaces. Concentrating collectors requires large reflectors [4] to 'concentrate' the incident solar radiation onto a smaller receiver. An assembly of mirrors [5,6] is required to reflect and to focus the sunlight onto a receiver containing a heat transfer fluid (HTF), such as molten salt, steam, oil, compressed air [7] etc. The hot fluid is then utilized to produce electric power through standard steam turbines [8].

Reflectors are an essential part of CSP systems and considerable amount of research has been devoted in the development and improvement of reflector materials. [9,10] Reflectors in CSP systems [11] require a high reflectance over the entire solar spectrum, durability to outdoor exposure and resistant to all forms of degradation over time, particularly from humid conditions and dust in order to improve their lifetime in adverse environment of the solar fields [12]. Most of the large-scale CSP systems, installed till now, utilize glass reflectors [13]. Although these mirrors have maintained their reflectance very well in severe environments, they are prone to wind-related breakage and are expensive to transport and install. In order to overcome this issue, immediate attention is required for alternative lower-cost reflectors to reduce the cost of CSP systems.

From a variety of different material constructions, the mirror materials showing promise for long-term outdoor applications, [14] are reported to be made up of various silvered glass mirrors [15], a silvered polymeric mirror [16], and an anodized sheet

aluminium [17] with an additional protective polymer coating. Comparative optical tests [18] were carried out and reported earlier on these materials, mainly to correlate the efficiency as a function of exposure/ service time in a solar concentrator [19]. With the above backdrop, research based on developing newer reflector materials with inherently high specular reflectance and corrosion resistance has attained a greater significance in recent times. [20,21] For example, SolarBrite 95, [22] developed commercially by Alcoa, consisted of a silvered ultra violet (UV)-stabilized polyester film having a metallic back-protective layer. However, the samples exhibited poor durability and in particular the UV stabilized polyethylene terephthalate (PET) yellowed after 8 months of accelerated exposure and 20 months outdoors at the National Renewable Energy Laboratory (NREL). Recently, Almeco solar [23] have developed composite mirror manufactured using highly reflective weather resistant aluminium layer of 99.99% combined with a plastic core and a corrosion resistant stabilizing aluminum sheet on the backside. This consists of reflection enhancing system made of pure aluminium layer deposited by PVD technique surmounted by two transparent optical layers of alternate low and high refractive index materials to enhance reflectance property.

One interesting and relatively cost effective and faster way to develop thin films with high reflectance is by electrochemistry [24]. Electrodeposition [25] is the process of electrochemically coating a thin layer of one metal on top of a different metal to modify its surface and optical properties. It is one of the most economical methods known for obtaining lustrous coatings. Furthermore, electrodeposition is scalable and hence provides a promising approach to obtain large area coating of reflector materials. Investigations aimed for developing electroplating baths, to produce bronze coatings of high quality are of great interest [26]. Sulfate bronzing electrolytes that are less toxic and low-priced, completely meet the process requirements for operating at room temperature and are considered to be the most

promising materials today. Bronze plating solution containing Laprol 2402C (product of polycondensation of ethane and propene oxides with average molecular mass of 3200) has been reported previously. [27] It is known aforesaid that the phase composition of electrodeposited alloys usually differs from that of the metallurgical ones [28], since electrodeposition does not occur under equilibrium conditions [29]. Further, it is possible to alter the kinetics of an electrodeposition process using suitable surfactants [30]. Motivated with this, we are reporting the electrodeposition of high-temperature, non-equilibrium δ phase intermetallic mirror coatings for solar reflector application.

In a recent publication, we have shown that Cu-Sn intermetallic alloys, corresponding to the intermetallic δ phase, possess high specular reflectance of $> 80\%$. Together with good mechanical properties and wear resistance, this can be a potential material for CSP mirror. [31,32] We argue that this alloy, if successfully coated on mild steel, can lead to the development of scratch resistant solar mirror for dusty and environmentally harsh locations. The lustrous coatings can be electrodeposited galvanostatically from acidic sulfate based electrolyte in the presence of Laprol as an additive. [33] Optimized Cu-Sn co-deposition can be obtained by systematic changes in the deposition conditions, such as applied current, bath composition and time of deposition. In this paper, we report the relationship among the phase compositions, surface morphology, thickness and surface coverage of this novel coating on mild steel and evaluate properties such as scratch hardness and scratch adhesion, resistance to tarnishing, effect of dust and humidity which are important for CSP applications.

2. Experimental

Copper-rich Cu-Sn alloys were electrodeposited on mild steel substrate from the electrochemical bath containing $\text{CuSO}_4 \cdot 5\text{H}_2\text{O}$ (Sigma Aldrich, $\geq 98.0\%$), SnSO_4 (Sigma Aldrich, $\geq 95\%$), H_2SO_4 (AR grade), and laprol 2402 C (Sigma Aldrich). All solutions were prepared using distilled water. The temperature of the solutions was maintained at 20 ± 1 °C.

The Mild steel is purchased locally and Aluminium is purchased from LOBA CHEMIE PVT.LTD, Mumbai. The electrodeposition experiments were carried out using mild steel (15mm*30mm*0.5mm) as working electrode. To obtain desirable surface roughness, the working electrodes were prepared by a mechanical polishing process using emery polishing paper and diamond paste of 0.1 μ m. The electrical contact was established by spot welding copper wire onto mild steel.

Electrochemical measurements were performed using Autolab PGSTAT 302N (Metrohm Autolab electrochemical instruments, Switzerland), with a conventional three-electrode system. The cyclic voltammogram for electrochemical bath composition was carried out using glassy carbon working electrode, glassy platinum counter electrode and Ag|AgCl|KCl (3M) ($E^0 = + 0.210$ V vs normal hydrogen electrode (NHE)) as reference. For electrodeposition, chronopotentiometry (constant current) was performed. The platinum electrode (30mm*12mm*1mm) was used as the counter electrode and Ag|AgCl|KCl (3M as reference. All potentials were measured and reported with respect to this reference electrode unless until mentioned otherwise. The solutions were deaerated by bubbling nitrogen of 99.999% purity for 1 minute prior to use. All experiments were carried out at room temperature without stirring the electrolyte. The preliminary optimization was carried out galvanostatically at different currents to obtain the δ phase composition in the coating. Subsequently, the depositions were carried out for different time intervals at a fixed current to optimize the desired thickness.

X-ray diffraction patterns were obtained using an X-Ray diffractometer (XRD, PANalytical, Xpert pro) with CuK $_{\alpha}$ radiation ($\lambda = 1.5406$ Å), for identifying the phases present in the coatings. In general, XRD data were acquired at a scan rate of 0.5 $^{\circ}$ /min. The structural properties of the films were studied by computer controlled RIGAKU, X-ray diffractometer using CuK $_{\alpha}$ (1.5406 Å) radiation. The scanning angle was varied from 10 to

90° in step of 0.24° /sec. For metallography, the samples were etched using acidified potassium dichromate [32,34] and subsequently colour tinted using reagent based on complex thiosulphate solution. As part of the microstructural investigation, intermetallic coatings were characterized using scanning electron microscope (SEM) (FEI Corporation, Netherlands) equipped with energy dispersive spectrometer (EDS) for various microstructural and compositional analysis. The surface morphology of the Cu-Sn coating was studied using atomic force microscope (AFM) (Nanosurf easy scan 2, Nanosurf Inc., USA). The thickness of the coating was measured using non-contact optical profilometer (CCI MP TalySurf, Ametak, UK). Specular reflectance was measured at 8° incident angle and 20 nm slit width using UV-Visible-NIR integrating sphere spectrophotometer (Perkin Elmer Lambda 950 with Universal Reflectance Accessory attachment, USA). The contact angle measurements were performed using contact angle goniometer OCA 15EC (Video based contact angle measuring unit with software SCA 20, DataPhysics Instruments, Germany).

A custom-made laboratory set-up was utilized for testing the effect of humidity on coatings. In this set-up, the temperature was set at 50°C and relative humidity ~ 90% for a period of 3 days and any variation was continuously recorded using fluke 971 temperature humidity meter. To measure the effect of dust [3] on specular reflectance of different mirror materials under the existing climate of Bengaluru, India (12° 58' N, 77° 38' E), the as-deposited Cu-Sn coatings, mild steel and aluminum coupon were mounted on roof top adjacent to solar cells at two different angles 0° and 14.5°. Specular reflectance measurements of these samples were acquired before and after exposure to humidity. The decrease in specular reflectance was determined by calculating the reflectance variation, $\Delta\rho$. [36]

Scratch hardness test was conducted using Hysitron TI 950 TriboIndenter (Hysitron Inc., USA). A Berkovich probe of radius of curvature 150 nm was used for indenting loads from 0.5 mN to 10 mN loads. Scratch adhesion test was performed with nano scratch tester

(Bruker's Scratch Test System, USA). For scratch adhesion, a 200 μm tip radius Rockwell diamond indenter is moved over a specimen surface of 1mm at a speed of 0.02mm/s, with a linearly increasing load from 1 N to 4.5 N.

3. Results and Discussion

For potentiometric experiments, hypoeutectoid mild steel was chosen as the working electrode. The XRD pattern of substrate (figure 1) matches with that of Fe (JCPDS Card No: 04-002-8917) having bcc crystal structure. The SEM microstructure of the substrate is shown in figure 2.

The electrochemical bath for Cu-Sn alloy deposition was optimized and contained $0.03 \text{ mol dm}^{-3} \text{ CuSO}_4 \cdot 5\text{H}_2\text{O}$, $0.01 \text{ mol dm}^{-3} \text{ SnSO}_4$, $0.6 \text{ mol dm}^{-3} \text{ H}_2\text{SO}_4$ and 50 mg dm^{-3} laprol 2402 C. The cyclic voltammetry was performed without Laprol additive, at a scan rate of 10 mV/s in three successive cycles for electrochemical characterization of Cu-Sn bath as shown in figure 3. The process was carried out using glassy carbon working electrode, glassy platinum counter electrode and Ag|AgCl|KCl (3M) ($E^0 = + 0.210 \text{ V}$ vs normal hydrogen electrode (NHE)) as reference electrode. The reduction potential and oxidation potential of the electrolyte solution were found to be -0.173 V and $+0.184 \text{ V}$ vs Ag/AgCl, respectively. The constant current plot at -8.5 mA , exhibiting the relationship of potential with time of deposition is shown in figure 4. A constant steady potential of -0.58 V was obtained within 50 seconds of chronopotentiometry for deposition.

The plating bath solution was prepared with an acidic pH of 0.6 and the bath composition was standardized for obtaining δ phase in the film which was confirmed by performing XRD of as-deposited coatings. The X-ray pattern of the electrodeposited working electrode with the above bath composition is shown in figure 5. The patterns obtained from coating can be completely indexed with the reflections of the δ phase (JCPDS Card No: 01-071-0094). The electrodeposition was carried out galvanostatically by varying current to

achieve lustrous reflective films, as shown in figure 6. The optimised reflective surface containing δ phase in the Cu-Sn alloy was achieved at an optimized current of -8.5 mA.

The SEM microstructure of the chemically etched Cu-Sn coating, obtained after 300 seconds of deposition is shown in figure 7. Consistent with the X-ray diffraction results, the microstructure indicates a single phase structure with some residual porosity. The composition homogeneity of the δ phase could be determined by performing the compositional analysis at multiple points. The composition analysis using EDS is shown in table 1. The composition of the phase was found to be around 65 % Cu and 35% Sn with an instrumental error ± 2 %. In order to understand the nature of the film further, cross-section of the film was studied using SEM. Figure 8 shows a typical cross sectional image. The microstructure shows a clear evidence of columnar growth of δ phase during the deposition process. Thus, the growth interface is not smooth and has corrugation at the vapor/solid interface. The porosity observed in the top section therefore pertains to these inter-columnar regions. The thickness of the as-deposited coating was measured to be ~ 2.7 μm . The summary of electrodeposition experiments that were performed by varying time is summarized in table 1.

In order to understand the reflecting surface better, the surface morphology of the Cu-Sn coating was obtained using AFM. This is shown in figure 9. The area roughness parameters with arithmetic average of absolute values (Sa) and root mean squared (Sq) values of the Cu-Sn coating was found to be 14.73 nm and 20.83 nm, respectively. The area roughness parameters (Sa and Sq) give more significant values to measure the surface roughness over an area. The Sa and Sq values confirm that surface of the film has acceptable roughness for reflector application. However, further scope exists for optimization by further control of growth conditions. Thickness of as-deposited film after 300 seconds was found to be ~ 2 μm (figure 10).

The specular reflectance spectra of the films with varying deposition times are presented in figure 11a. The specular reflectance of the Cu-Sn films is higher than the substrate and exhibit a linear relationship with increasing deposition time and consequently with increasing film thickness. The relationship between thickness and specular reflectance is shown in figure 11b. The specular reflectance of the film deposited in 300 sec was found to be the highest, the value being ~79 %. Beyond 360 sec, the film was darkened due to vigorous reaction at the substrate-electrolyte interface.

The wettability of the surface of a CSP reflector plays significant role for efficient cleaning and the dust deposition. We have, therefore, evaluated the wetting behaviour of the surface by droplet technique. The morphology of the water droplet on the coating is shown in figure 12. The contact angle is measured to be 109° , that indicates the hydrophobic nature of the coatings. This suggests lesser dust deposition and easier cleaning particularly in a humid condition. For comparison, the water droplet contact angle on the polished and unpolished aluminium surface is 62° and 5° respectively, indicating strong hydrophilic nature [35]. Thus, Cu-Sn coating on mild steel may be more desirable for outdoor exposure than aluminium due its hydrophobic behaviour.

Further evaluation has been carried out to assess the performance of Cu-Sn reflectors coated reflectors in the hot and humid conditions. The coatings were subjected to a humidity test in a custom-made laboratory set-up, where the temperature was set to 50°C and the relative humidity was set at ~90% for a period over 3 days. The specular reflectance was measured before and after the exposure to estimate the effect of above conditions on the reflectance property of the deposited films. A summary of the results from humidity studies is shown in table 2. The Cu-Sn films exhibited a specular reflectance variation of 8.55 %, which is far better than aluminium showing a variation of 36.51% under the similar conditions. This

is attributed to the fact that at high temperature and high humidity, aluminium forms a native oxide layer which is dark and non-reflective whereas the Cu-Sn coating has negligible effect.

We have also studied the rate of dust deposition [36] on different mirror materials [3] a) as-deposited Cu-Sn coatings, b) reference mirror material, such as aluminum, and c) bare substrate mild steel in the climate of Bengaluru, India ($12^{\circ} 58' N$, $77^{\circ} 38' E$). For this purpose, mirrors were mounted on roof top at two different angles 0° and 14.5° . A summary of dust accumulation is presented in table 3. The deposition of dust on the Cu-Sn reflector is more compared to aluminium at 0° angle while it is less when the substrate is at an angle of 14.5° .

To evaluate the resistance of the reflectors to wear, scratch hardness test was performed with constant normal load on the coating starting from 0.5 mN to 10 mN. The test was conducted on both coated and uncoated mild steel for comparison. The relationship between applied load and hardness of Cu-Sn film is shown in figure 13a. The penetration depth Vs indentation force is shown in figure 13b. The coating exhibited better hardness of 7 GPa at 2 mN load as compared to the substrate hardness of 4.2 GPa under similar loading. At 10 mN applied load, coating exhibited a hardness of 2.6 GPa, which enables the coatings to be classified as durable.

Furthermore, scratch adhesion test was performed on the coatings. It is one of the widely used, fast, and effective methods to obtain the critical loads that are related to adhesion properties of coating. This test was performed by applying a linearly increasing load from 1 N to 4.5 N to determine the adhesion of the coatings. Acoustic Emission (AE) is also measured during the test. Acoustic emission indicated the absence of fluctuations, confirming that the coating is well adhered till 4.5 N load. Each scratch was examined with an optical microscope for the onset of cracking. The optical micrograph of the scratch is shown in figure 14, where no crack is visible in the entire scratch length. This observation confirms that the

coating can withstand a load of 4.5 N or above, indicating that the Cu-Sn deposit is well adhered to the substrate.

At the closure, the relevance of the present work in the context of commercialization needs to be looked into. In recent times, large scale production of mirror is mainly dependent on physical vapor deposition (PVD) technique. However, main disadvantage of coating PVD is higher costs that result from expensive instrumentation, intricate infrastructure and the need for skilled manpower. Also, PVD coating operations are relatively slower process and not time efficient. In the above perspective, cost-effective viable method for mirror development is essential for the maintenance of CSP system. To this end, the results of the present work suggest that it is possible to electrochemically deposit reflector materials based on Cu-Sn intermetallic alloys on mild steel substrates. The coating thickness as well as the morphology of the coating microstructure needs to be refined in order to enhance the specular reflectance. In particular, the electrochemical deposition conditions needs to be tailored to facilitate plane front growth of the coating microstructure, which is expected to be beneficial in improving reflectance. An additional approach can be to deposit another coating of high refractive index on the top of the Cu-Sn coatings to enhance the reflectance in the UV-Vis range. All these approaches will be pursued in our future research.

The reflector materials needed in CSP plants should ideally last for 20 to 30 years and the manufacturing cost should be less than \$2.50 per square foot (or \$25 per square meter) [37]. In the present work, the cost structure is calculated to estimate the viability of our coatings. From the above calculations, Rs 30000/- (\$500) is considered for electrodepositing 100 mild steel (MS) sheet (1m*1m) with Rs 300/- (\$5) per square meter for coating each MS sheet, which is considered to be more economical than the current scenario.

4. Conclusion

In summary, we have developed a reflecting Cu-Sn intermetallic alloy of predominantly single phase $\text{Cu}_{41}\text{Sn}_{11}$ based mirror material using electrodeposition on mild steel substrate with specular reflectance of ~80%. Microstructurally, the reflector consists of intermetallic δ phase that was obtained by electrodeposition. The formation of δ phase has been confirmed by XRD and EDS analysis. SEM studies indicate a columnar growth and uniform surface coverage with coating thicknesses of ~ 2 μm . AFM roughness studies revealed a relatively smooth film with roughness in the nano range. Mechanical properties of these alloy coatings such as scratch hardness and scratch adhesion were studied to ensure that the new coating avoids failure in the real field conditions. The effect of humidity (90% RH) and dust were also reported to assess the optical requirements of this new material as a reflector for solar concentrators.

Acknowledgement

This research is based upon work supported by the US-India Partnership to Advance Clean Energy-Research (PACE-R) for the Solar Energy Research Institute for India and the U.S. (SERIUS) funded jointly by the U.S. Department of Energy subcontract DE AC36-08G028308 (Office of Science, Office of Basic Energy Sciences, and Energy Efficiency and Renewable Energy, Solar Energy Technology Program, with support from the Office of International Affairs) and the Government of India subcontract IUSSTF/JCERDC-SERIUS/2012 dated 22nd Nov. 2012.

The authors also appreciate the help rendered by Dr Harish C. Barshilia, National Aerospace Laboratory, Bengaluru for the measurement of specular reflectance and scratch adhesion test.

References

- [1] J. Polo, F.M. Téllez, C. Tapia, Comparative analysis of long-term solar resource and CSP production for bankability, *Renewable Energy*, 90 (2016) 38-45 .
- [2] E. M. Toygar, T. Bayram, O. Daş, A. Demir, The design and development of solar flat mirror (Solarux) system, *Renewable and Sustainable Energy Reviews*, 54 (2016) 1278–1284.
- [3] T. Sarver, A. Al-Qaraghuli, L. L. Kazmerski, A comprehensive review of the impact of dust on the use of solar energy: History, investigations, results, literature, and mitigation approaches, *Renewable and Sustainable Energy Reviews*, 22 (2013) 698–733.
- [4] N. Lior, Mirrors in the sky: Status, sustainability, and some supporting materials experiments, *Renewable and Sustainable Energy Reviews*, 18 (2013) 401–415
- [5] M. Wang, R. Vandal, S. Thomsen, Durable concentrating solar power, *Guardian Industries Corp*, Carleton, USA, 1-5.
- [6] R. B. Pettit, E. P. Roth, Solar Mirror Materials: Their Properties and Uses in Solar Concentrating Collectors, in *Solar Materials Science*, L. E. Murr, ed., Academic Press, New York, (1980) 171-197.
- [7] Zhuo Li, Zhi-Gen Wu, Analysis of HTFs, PCMs and fins effects on the thermal performance of shell–tube thermal energy storage units, *Solar Energy*, 122 (2015) 382-395.
- [8] M. Montecchi, Approximated method for modelling hemispherical reflectance and evaluating near-specular reflectance of CSP mirrors, *Solar Energy*, 92 (2013) 280-287.
- [9] M. DiGrazia, R. Gee, G. Jorgensen, ReflecTech Mirror Film Attributes and Durability for CSP Applications, *ASME 2009 3rd International Conference on Energy Sustainability*, San Francisco, California, USA,2 (2009) 677-682.

-
- [10] C. T. Kutscher, R. Davenport, Preliminary Results of the Operational Industrial Process Heat Field Tests, SERI/TR-632-385R, Solar Energy Research Institute, Golden, CO, June (1981).
- [11] C. Delord, C. Bouquet, R. Couturier, O. Raccurt, Characterizations of the durability of glass mirrors for CSP Development of a methodology, Solar PACES; 2012.
- [12] K. D. Bergeron, J. M. Freese, Cleaning Strategies for Parabolic Trough Collector Fields; Guidelines for Decisions, SAND81-0385, Sandia National Laboratories Albuquerque, 1981.
- [13] Huawei Chang, Chen Duan, Ke Wen, Yuting Liu, Can Xiang, Zhongmin Wan, Sinian He, Changwei Jing, Shuiming Shu, Modeling study on the thermal performance of a modified cavity receiver with glass window and secondary reflector, Energy Conversion and Management, 106 (2015) 1362-1369.
- [14] T. Fend , B. Hoffschmidt, G. Jorgensen, H. Kuster, D. Kruger, R. Pitz-Paal, P. Rietbrock, K. Riffelmann, Comparative assessment of solar concentrator materials, Solar Energy, 74 (2003) 149–155.
- [15] F. Sutter, A. Fernández-García, P. Heller, K. Anderson, G. Wilson, M. Schmücker, P. Marvig, Durability Testing of Silvered-Glass Mirrors, Energy Procedia, 69 (2015)1568-1577
- [16] Yuan Liao, Bing Cao, Wen-Cai Wang, Liqun Zhang, Dezhen Wu, Riguang Jin, A facile method for preparing highly conductive and reflective surface-silvered polyimide films, Applied Surface Science, 255 (19) (2009) 8207-8212.
- [17] Maria Brogren, Anna Helgesson, Björn Karlsson, Johan Nilsson, Arne Roos, Optical properties, durability, and system aspects of a new aluminium-polymer-laminated steel reflector for solar concentrators, Solar Energy Materials and Solar Cells, 82 (3) (2004) 387-412.

-
- [18] Z. Edfouf, M. Guerguer, O. Raccurt, Glass and polymeric mirrors ageing under different Moroccan weathers, an application for CSP power plants, *Energy Procedia*, 69 (2015) 1508 – 1518
- [19] T. Fend, K. Wenzel, Optical flux measurements in the mirrors focal area of a parabolic trough concentrator. In: G. Flamant, A. Ferrière, F. Pharabod, (Eds.), *Proceedings of the 9th SolarPACES International Symposium on Solar Thermal concentrating Technologies (STCT 9)*. EDP Sciences, Les Ulis Cedex A, France, (1999) 605–609.
- [20] Y.J. Xu, J.X. Liao, Q.W. Cai, X.X. Yang, Preparation of a highly-reflective TiO₂/ SiO₂/ Ag thin film with self-cleaning properties by magnetron sputtering for solar front reflectors, *Solar Energy Materials and Solar Cells*, 113 (2013) 7-12.
- [21] Y.J. Xu, Q. W. Cai, X. X. Yang, Y.Z. Zuo, H. Song, Z.M. Liu, Y.P. Hang, Preparation of novel SiO₂ protected Ag thin films with high reflectivity by magnetron sputtering for solar front reflectors, *Solar Energy Materials and Solar Cells*, 107 (2012) 316–321.
- [22] T. Fend, B. Hoffschmidt, G. Jorgensen, H. Kuster, D. Kruger, R. Pitz-Paal, P. Rietbrock, K. Riffelmann, Comparative assessment of solar concentrator materials, *Solar Energy*, 74 (2003) 149–155.
- [23] A. Fernández-García, M. E. Cantos-Soto, M. Röger, C. Wieckert, C. Hutter, L. Martínez-Arcos, Durability of solar reflector materials for secondary concentrators used in CSP systems, *Solar Energy Materials and Solar Cells*, 130 (2014) 51–63.
- [24] G. Zangari, Electrodeposition of alloys and compounds in the era of microelectronics and energy conversion technology, *Coatings*, 5 (2015) 195-218.
- [25] J. W. Dini, D. D. Snyder, *Modern Electroplating, Fifth Edition*, M. Schlesinger, M. Paunovic, John Wiley and sons, (2010) 33-78.

-
- [26] G. I. Medvedev, N. A. Makrushin, O. V. Ivanova, Electrodeposition of Copper-Tin Alloy from Sulfate Electrolyte, *Russian Journal of Applied Chemistry*, 77 (7) (2004) 1104-1107.
- [27] A. Survila, Z. Mockus, S. Kanapeckaitė, Voltammetric characterization of Laprol 2402 C adsorption on copper and tin electrodes, *Chemija*, 12 (4) (2001) 241-245.
- [28] S. D. Beattie, J. R. Dahn, Single Bath, Pulsed Electrodeposition of Copper-Tin Alloy Negative Electrodes for Lithium-ion Batteries, *J. Electrochem. Soc.*, 150 (7) (2003) A894-A898.
- [29] S. D. Beattie, J. R. Dahn., Single-Bath Electrodeposition of a Combinatorial Library of Binary $\text{Cu}_{1-x}\text{Sn}_x$ Alloys *J. Electrochem. Soc.*, 150 (7) (2003) C457-C460.
- [30] N. Pewnim, S. Roy, Electrodeposition of tin-rich Cu–Sn alloys from a methanesulfonic acid electrolyte, *Electrochimica Acta*, 90 (2013) 498-506.
- [31] K. P. Shah, The Iron-Iron Carbide equilibrium diagram, *The handbook on Mechanical maintenance*, 1-12
- [32] S. Alex, K. Chattopadhyay, B. Basu, Tailored specular reflectance properties of bulk Cu based novel intermetallic alloys, *Solar Energy Materials and Solar Cells*, 149 (2016) 66–74.
- [33] R. Juskenas, Z. Mockus, S. Kanapeckaitė, G. Stalnionis, A Survila, XRD studies of the phase composition of the electrodeposited copper-rich Cu–Sn alloys, *Electrochimica Acta* 52 (2006) 928–935.
- [34] N. N. Acharya, P. G. Mukunda, Metallography of copper-tin alloys, *Metallography*, 21 (1998) 137-150.
- [35] R. Sili, Y. Shengrong, Z. Yapu, Nani-tribological study on a super-hydrophobic film formed on rough aluminium substrates. *Acta Mechanica Sinica*, 20 (2) (2004) 159-164
- [36] D. J. Griffith, L. Vhengani, M. Maliage, Measurements of mirror soiling at a candidate CSP site, *Energy Procedia* 49 (2014) 1371 – 1378.

[37] Advanced Reflector and Absorber Materials, Thermal Systems Group: CSP Capabilities.

<http://www.nrel.gov/csp/pdfs/48662.pdf>

Figure 1 XRD pattern indicating Fe peaks for working electrode (mild steel).	23
Figure 2 SEM microstructure of working electrode (mild steel).	24
Figure 3 Cyclic voltammogram of Cu-Sn electrochemical solution containing 0.03 mol dm ⁻³ CuSO ₄ ·5H ₂ O, 0.01 mol dm ⁻³ SnSO ₄ and 0.6 mol dm ⁻³ H ₂ SO ₄	25
Figure 4 Potential Vs time plot for Cu-Sn co-deposition at constant current -8.5 mA.....	26
Figure 5 (a) GIXRD of Cu-Sn thin film obtained for 300 sec at a fixed current of -8.5 mA, (b) XRD for standard Cu ₄₁ Sn ₁₁ , (c) XRD of mild steel substrate.....	27
Figure 6 Photograph of as-deposited Cu-Sn alloy film showing a clear reflecting surface.	28
Figure 7 Etched microstructure of the Cu-Sn coating obtained at an applied current of -8.5 mA.	29
Figure 8(a) Sample edge exhibiting the columnar growth and (b) thickness of the deposits are indicated.....	30
Figure 9 AFM image showing the surface morphology of Cu-Sn coating.....	31
Figure 10 Optical profilometer measurements showing the thickness of the coating.	32
Figure 11 (a) Specular reflectance of the Cu-Sn films deposited galvanostatically at -8.5 mA. (b) Graph showing the direct relationship of thickness and specular reflectance.	33
Figure 12 Pictorial view of water droplet on Cu-Sn film, with measured contact angle of 109.6, as indicated in the figure.	34
Figure 13 (a) Plot of hardness variation with load for Cu-Sn film and mild steel, (b) graph showing penetration depth in Cu-Sn film.	35
Figure 14 Optical micrograph of progressive loading (1N to 4.5N) nano scratch adhesion test for Cu-Sn film.....	36

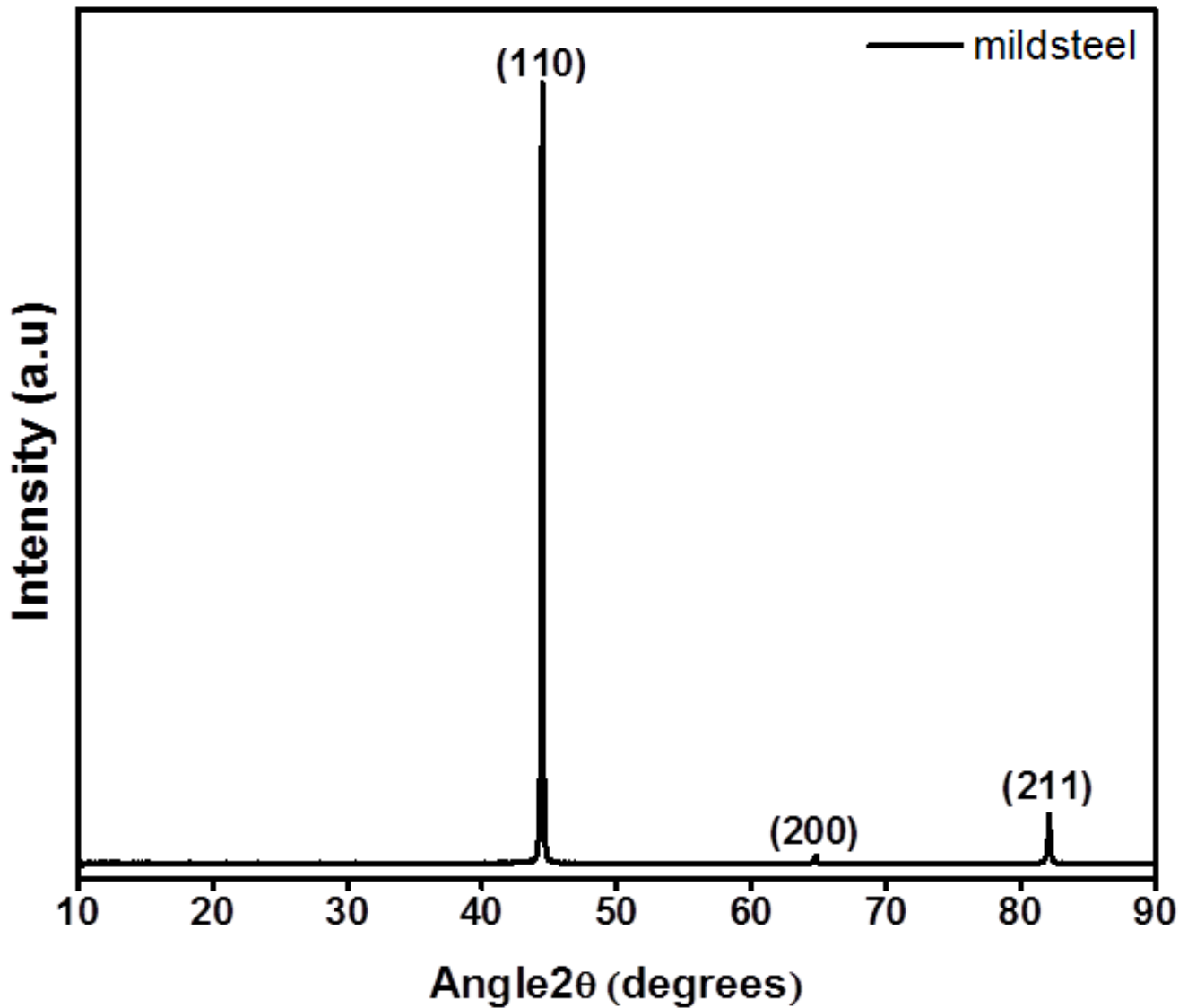


Figure 1 XRD pattern indicating Fe peaks for working electrode (mild steel).

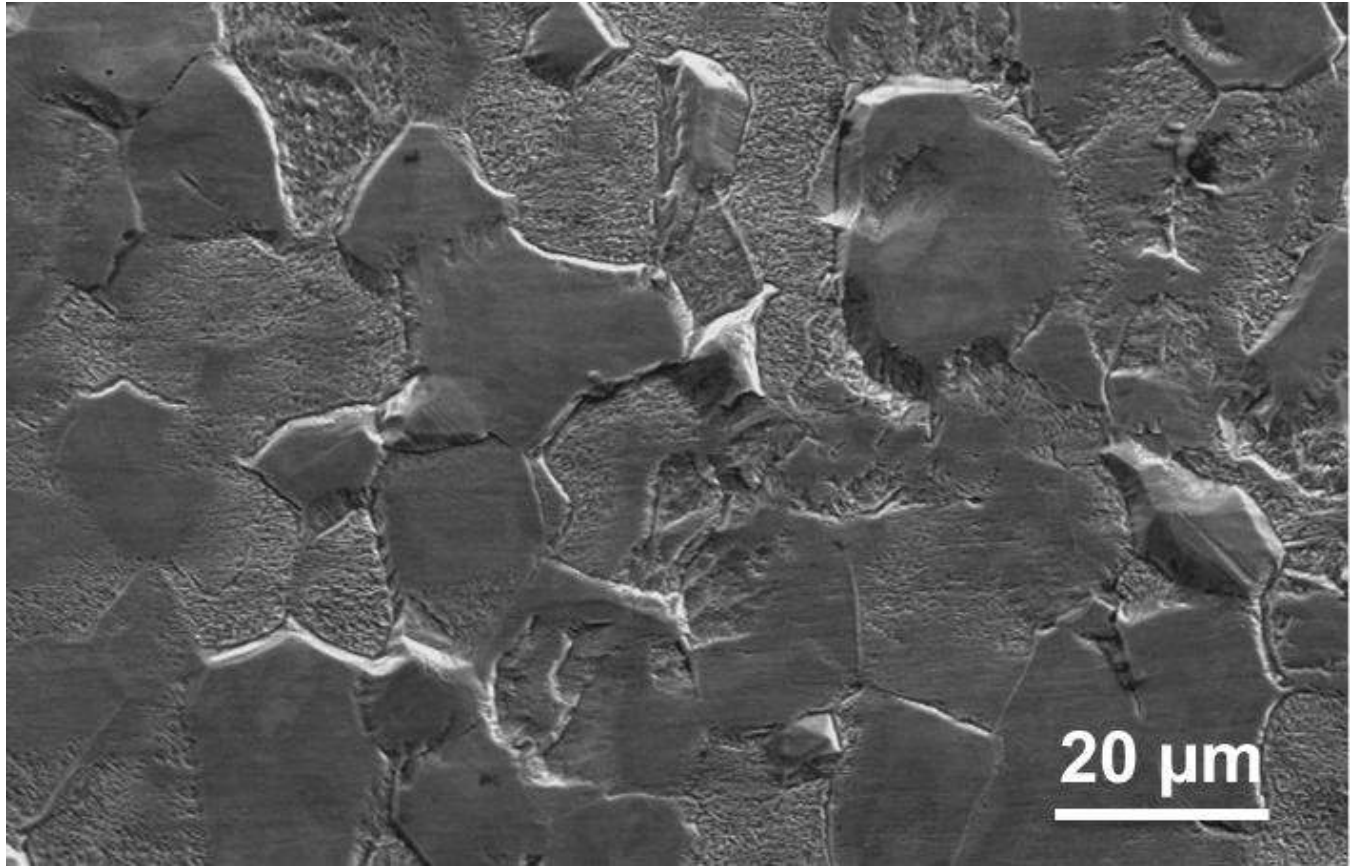


Figure 2 SEM microstructure of working electrode (mild steel).

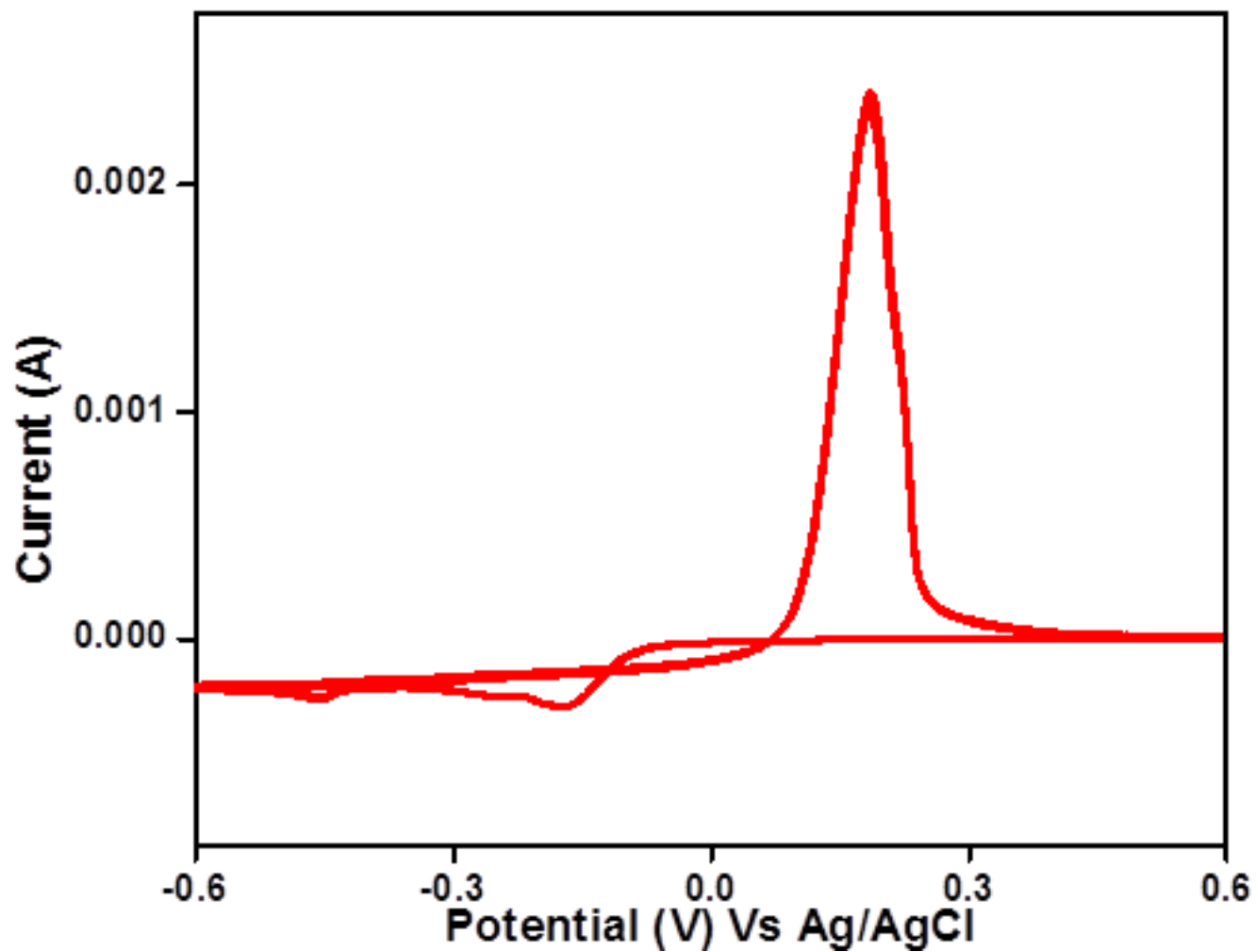


Figure 3 Cyclic voltammogram of Cu-Sn electrochemical solution containing 0.03 mol dm^{-3} $\text{CuSO}_4 \cdot 5\text{H}_2\text{O}$, 0.01 mol dm^{-3} SnSO_4 and 0.6 mol dm^{-3} H_2SO_4 .

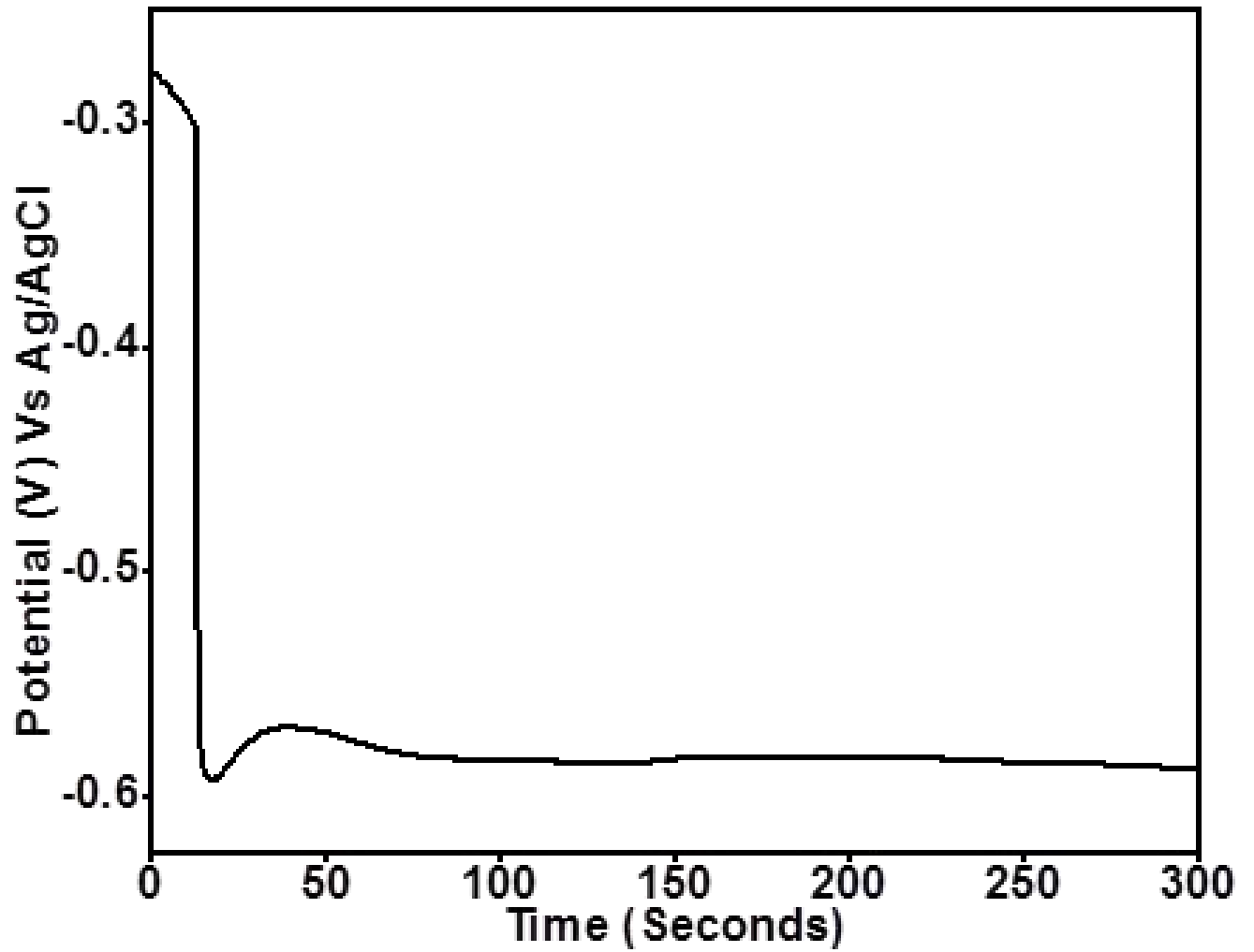


Figure 4 Potential Vs time plot for Cu-Sn co-deposition at constant current -8.5 mA.

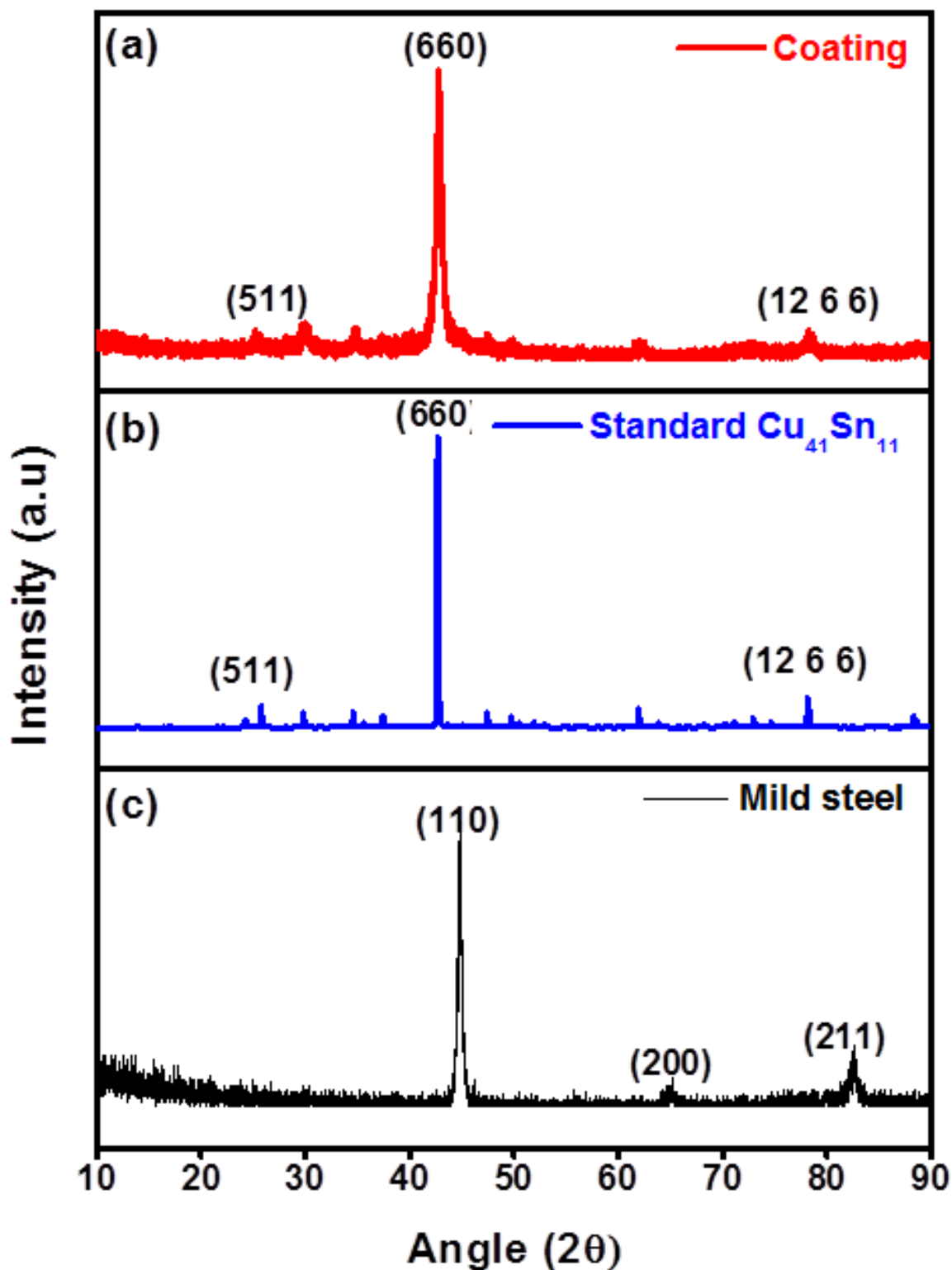


Figure 5 (a) GIXRD of Cu-Sn thin film obtained for 300 sec at a fixed current of -8.5 mA, (b) XRD for standard $\text{Cu}_{41}\text{Sn}_{11}$, (c) XRD of mild steel substrate.



Figure 6 Photograph of as-deposited Cu-Sn alloy film showing a clear reflecting surface.

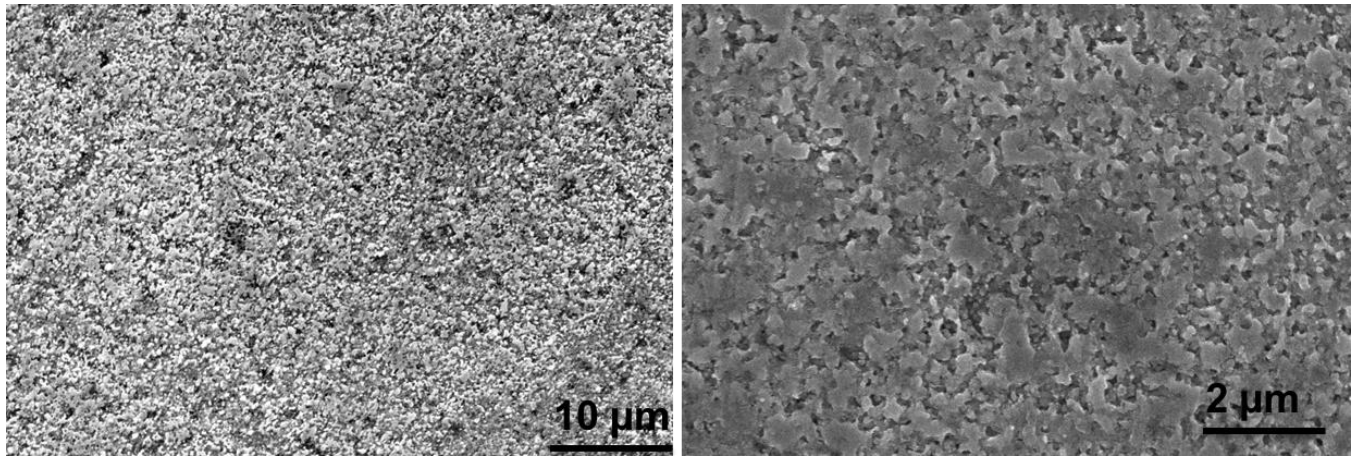


Figure 7 Etched microstructure of the Cu-Sn coating obtained at an applied current of -8.5 mA.

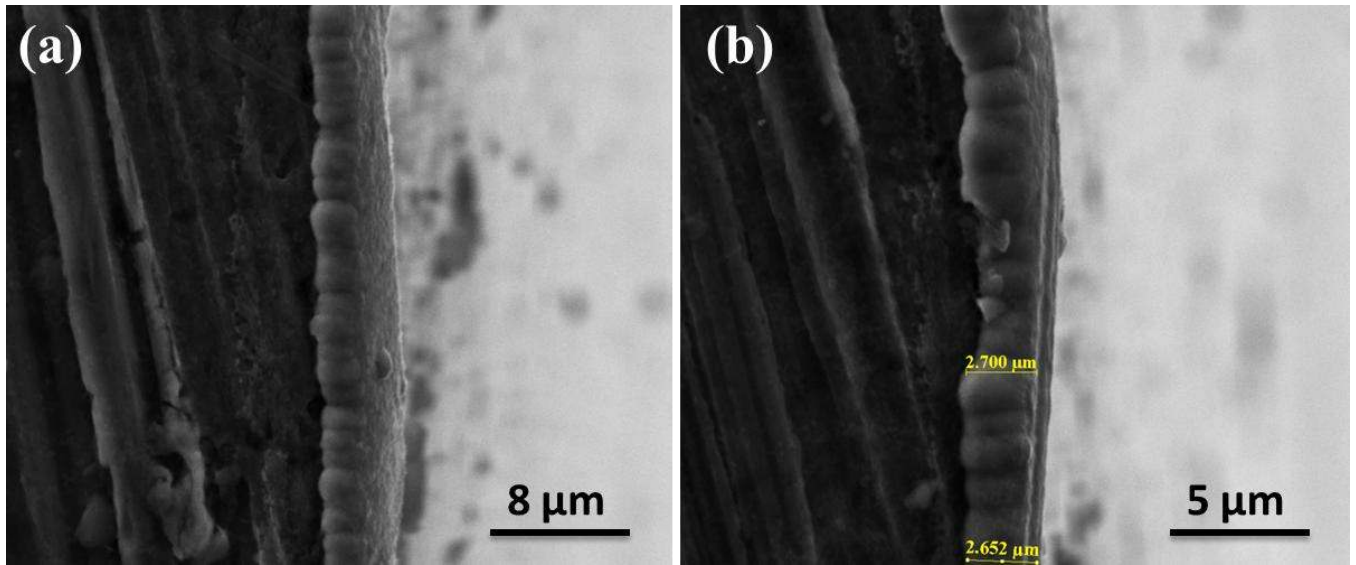


Figure 8(a) Sample edge exhibiting the columnar growth and (b) thickness of the deposits are indicated.

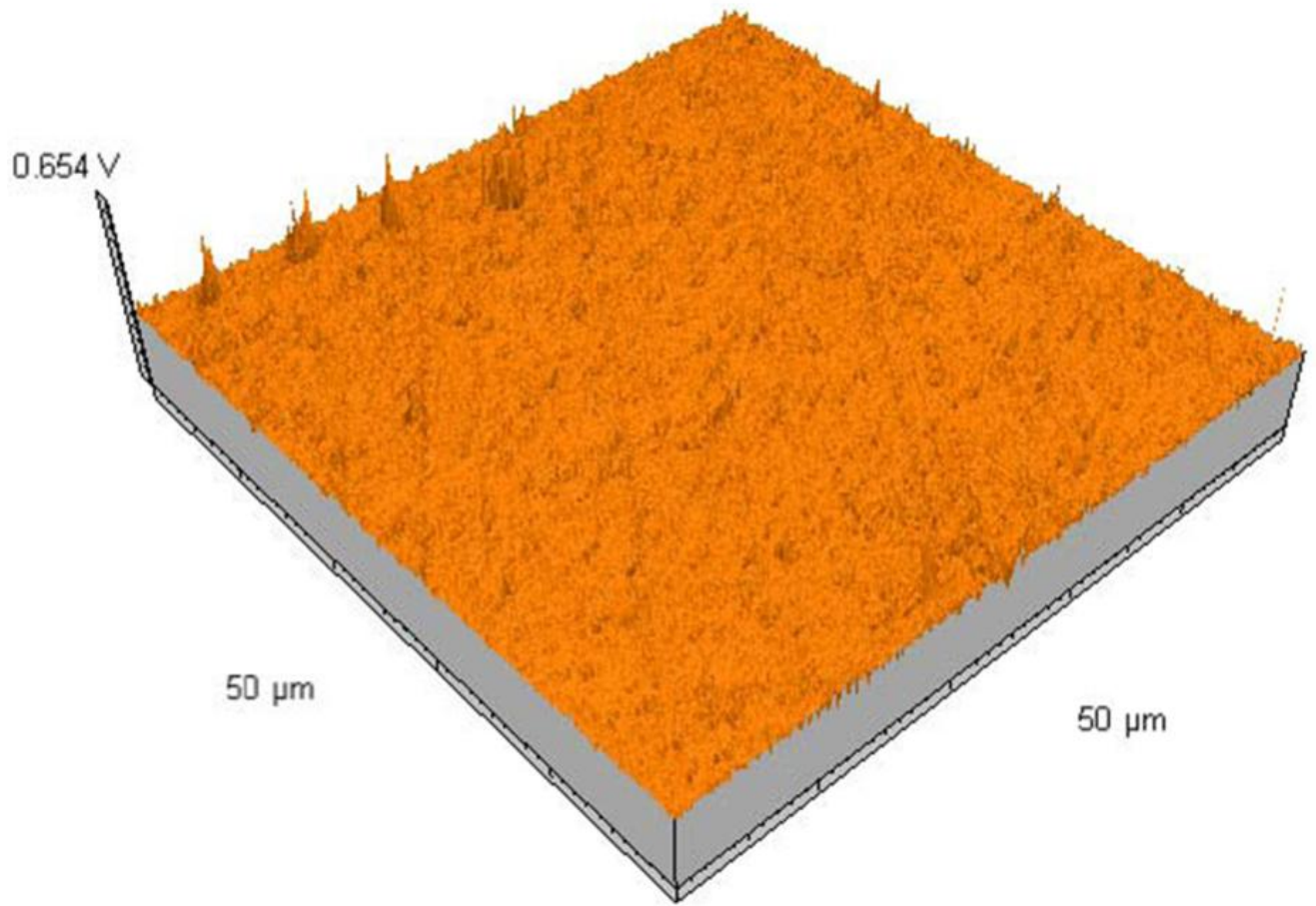


Figure 9 AFM image showing the surface morphology of Cu-Sn coating.

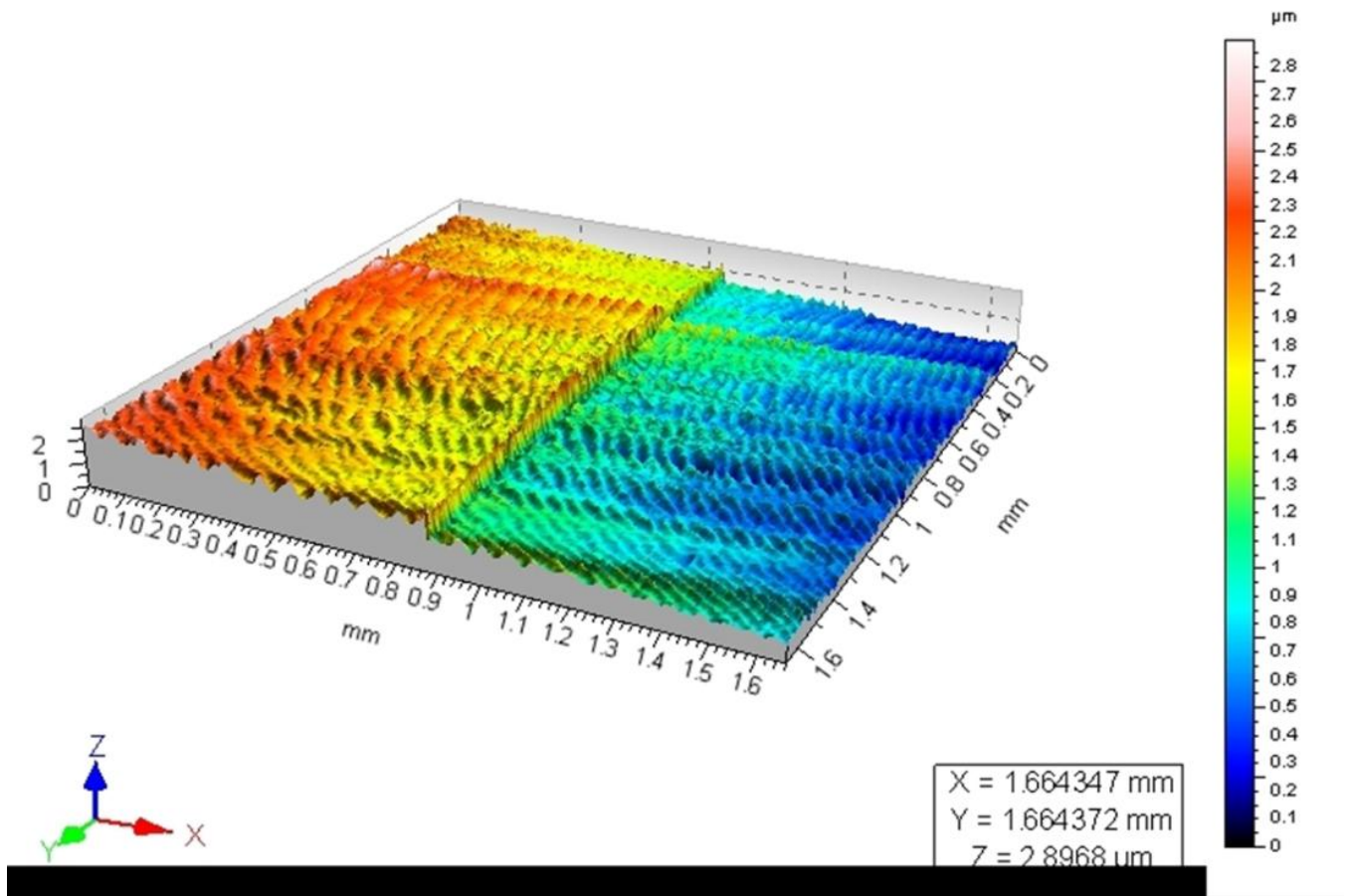


Figure 10 Optical profilometer measurements showing the thickness of the coating.

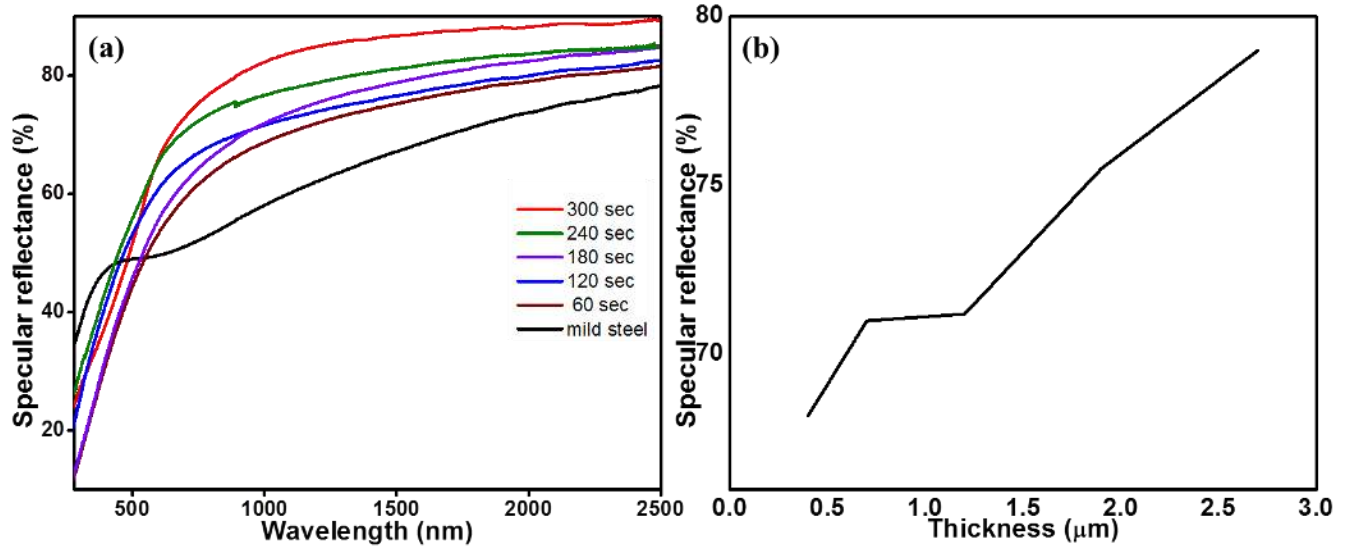


Figure 11 (a) Specular reflectance of the Cu-Sn films deposited galvanostatically at -8.5 mA. (b) Graph showing the direct relationship of thickness and specular reflectance.

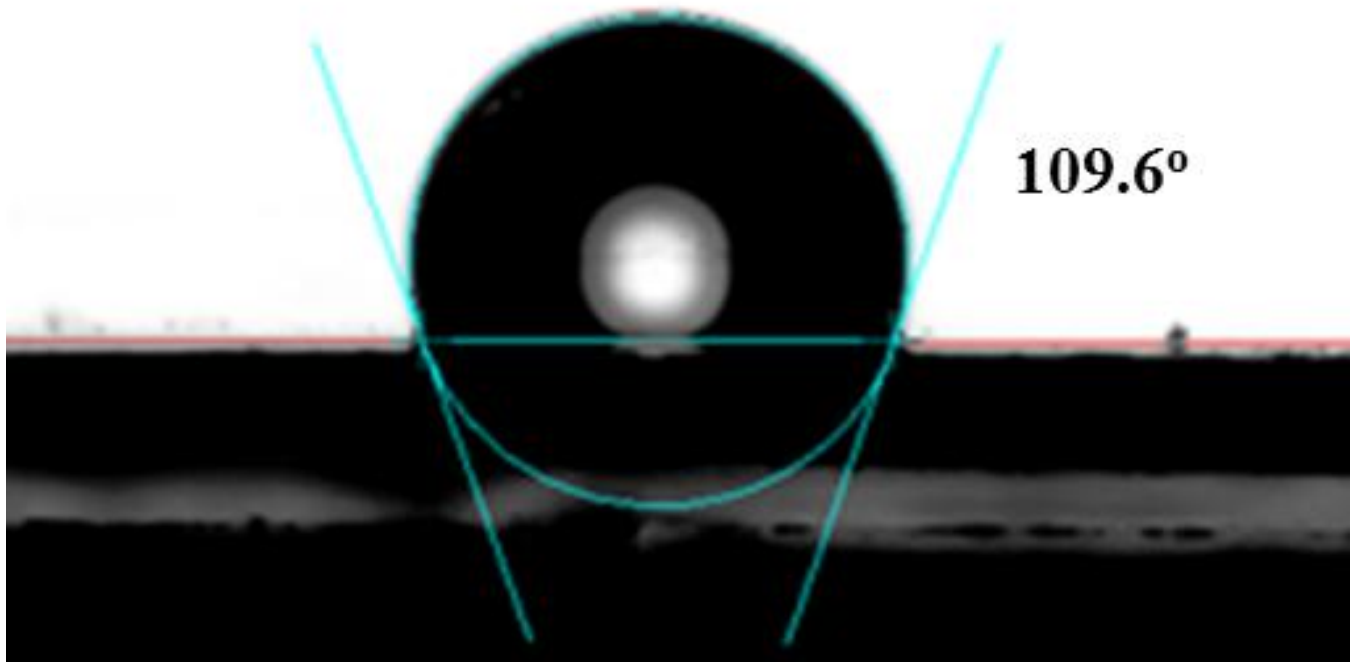


Figure 12 Pictorial view of water droplet on Cu-Sn film, with measured contact angle of 109.6, as indicated in the figure.

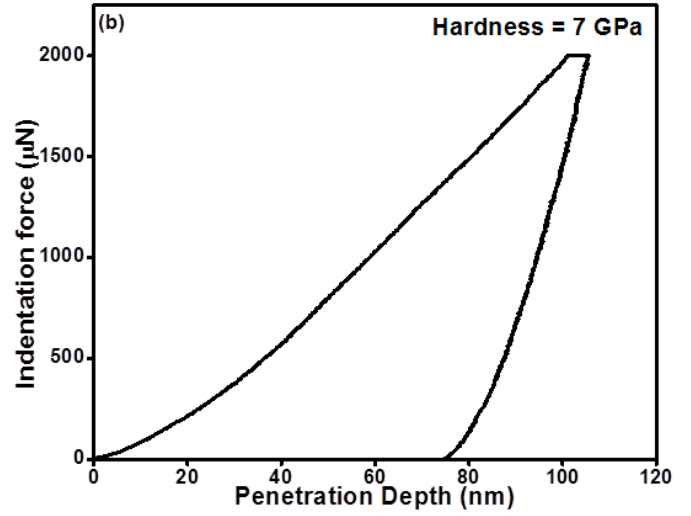
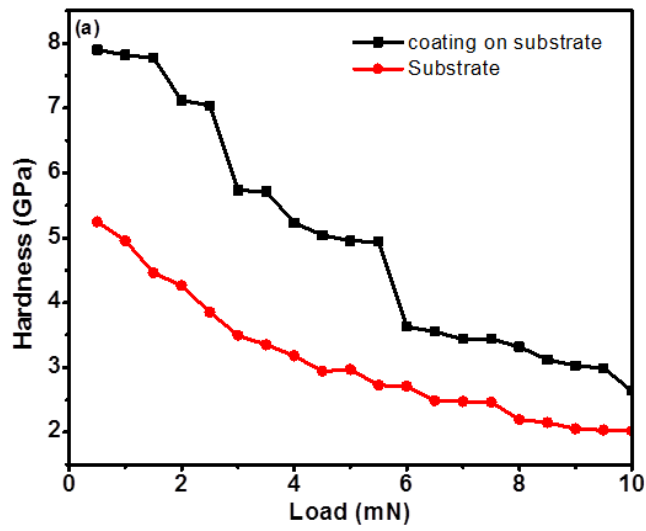


Figure 13 (a) Plot of hardness variation with load for Cu-Sn film and mild steel, (b) graph showing penetration depth in Cu-Sn film.



Figure 14 Optical micrograph of progressive loading (1N to 4.5N) nano scratch adhesion test for Cu-Sn film.

Table 1 Electrodeposition coating condition optimization and characterization.....	38
Table 2 Summary on humidity effects on reflectance of Cu-Sn thin film.....	39
Table 3 Summary of dust effects on the specular reflectance of Cu-Sn thin film.....	40

Table 1 Electrodeposition coating condition optimization and characterization.

Deposition Time (sec)	EDS (wt %)		XRD phase	Specular reflectance (%)	Thickness (μm)	Contact angle (degrees)
	Cu	Sn				
60	65	35	δ phase	68.2	0.4	108.7
120	66	34	δ phase	71	0.7	107.5
180	67	33	δ phase	71.2	1.2	108.3
240	65	35	δ phase	75.5	1.9	106.9
300	66	34	δ phase	79	2.7	109.6

Table 2 Summary on humidity effects on reflectance of Cu-Sn thin film.

Sample name	Specular reflectance (%)		Reflectance variation ($\Delta\rho$)
	before	after	
Cu-Sn film	76.93	67.84	8.55
Mild steel	63.44	63.37	0.07
Aluminium	45.87	9.36	36.51

Table 3 Summary of dust effects on the specular reflectance of Cu-Sn thin film.

Sample name	Angle of mounting, (degrees)	Weight of dust, (mg)		Weight difference, (mg)
		before	after	
Cu-Sn film	0	228.74	228.89	1.5
Mild steel	0	232.89	233.07	1.8
Aluminium	0	132.18	132.30	1.2
Cu-Sn film	14.5	236.98	237.15	1.7
Mild steel	14.5	260.14	260.33	1.9
Aluminium	14.5	130.45	130.67	2.2